Mechanical phenotyping of cells and extracellular matrix as grade and stage markers of lung tumor tissues

Mechanical Phenotyping of Cells and Extracellular Matrix as Grade and Stage Markers of Lung Tumor Tissues.

Valeria Panzetta[a], *Ida Musella*[a], *Ida Rapa*[b], *Marco Volante*[b], *Paolo A. Netti*[a,c], *Sabato Fusco**[,a]

[a] Istituto Italiano di Tecnologia, IIT@CRIB, L.go Barsanti e Matteucci 53, Naples, 80125, Italy

[b] Department of Oncology at San Luigi Hospital, University of Turin, Turin, Italy

[c] DCMIPE, University of Naples Federico II, 80125 Naples, Italy

Corresponding Author: sabfusco@unina.it L.go Barsanti e Matteucci, 53, Napoli – 80125 – Italy; Tel: +39 0811 9933100; fax: +39 0817 682404

Abstract.

The mechanical cross-talk between cells and the extra-cellular matrix (ECM) regulates the properties, functions and healthiness of the tissues. When this is disturbed it changes the mechanical state of the tissue components, singularly or together, and cancer, along with other diseases, may start and progress. However, the bi-univocal mechanical interplay between cells

and the ECM is still not properly understood. In this study we show how a microrheology technique gives us the opportunity to evaluate the mechanics of cells and the ECM at the same time. The mechanical phenotyping was performed on the surgically removed tissues of 10 patients affected by adenocarcinoma of the lung. A correlation between the mechanics and the grade and stage of the tumor was reported and compared to the mechanical characteristics of the healthy tissue. Our findings suggest a sort of asymmetric modification of the mechanical properties of the cells and the extra-cellular matrix in the tumor, being the more compliant cell even though it resides in a stiffer matrix. Overall, the simultaneous mechanical characterization of the tissues constituents (cells and ECM) provided new support for diagnosis and offered alternative points of analysis for cancer mechanobiology.

Keywords: Tumor mechanical phenotyping, Bioptic tissues, Extracellular matrix, Lung tumor, Multiple particle tracking

Introduction

The study of biomechanics and biophysics of cancer cells underlines the role of the components of the cellular cytoskeleton (CSK) in influencing some key functions such as cell mechanics, migration, differentiation, and neoplastic transformations [1-3]. In fact modifications to the CSK induced by external stimuli, such as chemical, topographic and mechanical gradients embedded in the extra-cellular matrix (ECM), act in concert with the tumorigenic molecular signalling to affect malignant transformations [4-6].

In comparison with healthy cells, biomechanical investigations reported some common features of many types of tumor cell lines, such as a less structured CSK [7-10] with lower cell mechanical [10-12] and cyto-adhesive properties [9, 10, 13, 14]. All factors which, from a biophysical point of view, augment the metastatic potential of the cancer cells [3, 7, 9, 14, 15]. However, most of the investigations performed *in vitro* focused on the mechanical state of the cell (both single unit and collective), neglecting the influence of the surrounding ECM. While cancer cells are more compliant than their healthy equivalents, the tissues affected by malignant tumors generally appear stiffer than healthy ones [11]. Therefore, for a very detailed mechanical phenotyping of tumors, it is necessary to consider the cross-talk between cells and their surrounding ECM. Tissue biomechanics is the result of a self-sustaining combination of interactions generating between cells and their micro-environments: i) cells may modify the environment chemically by metalloproteinase secretion [16, 17], or mechanically and topographically by generation and transmission of forces [18, 19]; ii) the ECM responsively adapts and, thanks to its mechanical and topographic features, is able to induce structural modifications in the CSK and to trigger different cell functions and behaviors. This closes the very intricate and complex loop of interactions existing between cells and ECM [20]. Hence the different mechanical characteristics of cancer cells which could arise either from an imprecise mimicking of their *in vitro* micro-environment, or from an insufficient resolution of the mechanical characterization at a sub-cellular and a sub-matricial level when tested *in vivo* or *ex vivo*. In fact many techniques which are used for the mechanical phenotyping of cells and tissues, like rheology or tissue elastography, suffer from poor spatial resolution and low force sensitivity.

In this work, human surgical tissue samples of lung adenocarcinoma, removed from 10 patients, were analyzed using the multiple particles tracking (MPT) technique with the aim of

mechanically phenotyping the tissues at cellular and ECM levels. A mechanical classification of the cells and the ECM of each sample was performed and compared with their healthy equivalents for all patients. Results and mechanical phenotypes were correlated to the stage and the grade of the tumor, previously assessed as part of the routine diagnostic procedure. In conclusion, we investigated and compared the ECM structure and morphology of both the tumor and the healthy tissues. This double-check mechanical characterization of *ex-vivo* biopsy tissues offers new diagnostic markers of the biophysical properties of the cells and the ECM (resolved at different spatial resolutions) and also gives new interpretative analytical points relating to cancer mechanobiology.

Methods.

Samples.

All experiments were performed in accordance with guidelines and regulations approved by the Research Ethics Committees of University of Naples and Turin. Experiments were performed on bioptic tissues from 10 patients with adenocarcinoma of the lung. One millimeter thick tumor tissue fragments (approximately 1 cm^2) were isolated from fresh surgical specimens by means of a sterile scalpel. Corresponding healthy tissue samples were collected from lung parenchyma at least 3cm away from the tumor nodule. After retrieval, tissue fragments were immediately prepared for cryopreservation as follows: samples were washed three times in a PBS buffer and transferred in 1.8 ml cryovials containing 1.5 ml of cryopreservation solution (RPMI 1640 medium supplemented with 10% foetal bovine serum and 10% DMSO). The cryovials were maintained at -20 °C for 1h and then stored at -80 °C.

Tissues were rapidly thawed in in a 37°C water bath and maintained in complete medium during particle tracking experiments.

Ballistic Injection and Particle Tracking Intracellular and Extracellular Mechanics.

Carboxyl-modified fluorescent polystyrene particles (0.50 μm diameter, Polyscience, Inc.) were introduced into the bioptic tissues using a ballistic gun (Bio-Rad, Hercules, CA). Helium gas at 2000psi was used to force a macro-carrier disk coated with particles to crash into a stopping screen. The force of collision was transferred to the particles, causing their dissociation from the macro-carrier and the bombardment of tissues. Once bombarded, tissues were washed extensively with phosphate-buffered saline (PBS, Lonza) and live cells were stained with DNA-specific dye, Hoechst 33342 (Life Technologies), at a 1:1000 dilution. Cell nuclei were stained in order to discriminate between cells and extra-cellular matrix (ECM) during optical microscopy analyses. The particles were considered inside the cells when they are in those zones in which the cells are packed and the contributions of the ECM can be neglected (see Supplementary Fig. 1, dotted blank square). Where this procedure was not feasible, we only considered those beads which are not more than 5 μm distant from the cell nuclei as belonging to the cells. Similarly, to consider particles inside the ECM, we took advantage of the collagen autofluorescence and looked at those zones in which nuclei are absent or their contribution is fringe (see Supplementary Fig. 1, dotted red square).After incubation, tissues were washed with PBS and the motion of intra-cellular and extra-cellular fluorescent beads was recorded for a total of 5 seconds at 100 frames per second (yielding a total of 500 frames per video) using a digital camera (Hamamatsu, ORCA-Flash2.8) attached to a PC and Cam control video capture software mounted on an inverted fluorescence microscope (Olympus IX81) equipped with a fluorescent

mercury lamp (Olympus U-LH100L-3). An oil immersion objective (100x, NA=1.40) at 1.6x magnification was used for particle tracking. Videos were kept short (the total duration was 5seconds) to avoid photo-bleaching of particles. To perform experiments under physiological conditions, a microscope stage incubator (Okolab, Naples, Italy) was used to keep cells at 37 °C and 5/95% CO_2/air mixture. The total number of analyzed particles was at least 200 from more than 20 cells and regions for each sample.

Particle tracking microrheology, introduced by Tseng *et al*. [21], allows the monitoring of local viscoelastic properties of living cells and the extra-cellular micro-environment with a high spatio-temporal resolution, collecting and analyzing the Brownian motions of particles embedded in cytoplasm and ECM, respectively. The particle displacements were tracked from the very beginning of the videos taken of beads embedded into the cells and ECM. To generate the point tracking trajectories, an ad hoc Matlab (Matlab 7) code performed two distinct steps: firstly it detected the beads in each frame, and then it linked the points into trajectories (see Supplementary Fig. 5). Each position was determined by intensity measurements through its centroid, and it was compared frame by frame to identify the trajectory for each particle, based on the principle that the closest positions in successive frames belong to the same particle (proximity principle). Once the nanoparticle trajectories had been obtained, mean squared displacements (MSDs) were calculated from equation (1)

$$\langle \Delta r^2(\tau) \rangle = \langle [x(t+\tau) - x(t)]^2 + [y(t+\tau) - y(t)]^2 \rangle \qquad (1)$$

where angular brackets mean time average, τ is the time scale and t the elapsed time. The particles embedded in regions with a thickness similar to or smaller than the particle diameter were excluded from the analysis (cell lamellar regions).

Tissue Morphology.

A Confocal Leica TCS SP5 II combined with a multi-photon laser source was used to investigate tissue morphology. To prepare them for observation under microscope the tissues were sliced. Because of the softness of the tissues they had to be embedded in Optimal Cutting Temperature (Killik, Bio-Optica). The tissues were first fixed in 4% paraformaldehyde (Sigma-Aldrich) in PBS for 20 minutes, rinsed twice with PBS and incubated overnight in 2M sucrose (Sigma-Aldrich) in distilled water. Afterwards the samples were embedded in OCT, snap frozen in liquid nitrogen, and stored at -80 °C. Next, the samples were sectioned at a thickness of 10 µm using a Cryostat (Leica CM 1850 UV), then mounted on coverslips and stored in the fridge (-20 °C) until staining. For actin microfilaments and nucleus detections, the samples were stained with Alexa 568- phalloidin (Life Technologies) and SYTOX Green (Life Technologies), respectively. The samples were permeabilized in 0.3% Triton X 100 (Sigma-Aldrich) in PBS for 5 minutes and then blocked in 10% bovine serum albumin (BSA, Sigma-Alderich) for 30 minutes to block unspecific binding. After blocking, samples were incubated for 1 hour with phalloidin at a 1:200 dilution in PBS-BSA. Finally, the samples were incubated with SYTOX Green diluted in PBS at 1:50000 for 10 min. Two-photon excited fluorescence was used to induce second harmonic generation (SHG) and obtain high-resolution images of the unstained collagen structures. Appropriate fluorescence filters were used: 504 nm excitation/523 emission for SYTOX Green,

578/600 for phalloidin. All the samples were imaged by two-photon excited fluorescence at λ_{ex} = 840 nm to induce SHG of unstained collagen structures by collecting the emission wavelength in the range λ_{em} = 420 ± 5 nm.

Immunohistochemical Analysis

Basal membrane material was highlighted by immunohistochemical detection of laminin (Novocastra; clone 4C7, diluted 1:50). A standard automated (Dako Autostainer, Glostrup, Denmark) immunoperoxidase procedure was employed, and immunoreactions were shown by a biotin-free dextran-chain detection system (Envision, Dako), and developed using diaminobenzidine as the chromogen.

Statistical Analysis

Data are reported as mean ± standard error (SE), unless otherwise indicated. Statistical comparisons were performed with a student's unpaired test. P values < 0.05 denote statistical significance.

Results and Discussion

To correlate the nanomechanical properties of lung tissue to its pathophysiological state, we performed particle tracking microrheology analyses of ex vivo lung tissues, distinguishing between cellular and ECM contributions. Polymeric nanobeads (500 nm) were introduced through a ballistic bombardment into the sample slice and tracked to obtain their motion across cell cytoskeleton and ECM structures. As has already been demonstrated [22], the amplitude and

the slope of mean square displacement (MSD) calculated from bead motion is inversely related to the mechanical properties of the intra-cellular and extra-cellular micro-environment. For this reason, we compared the MSDs of particles introduced in cytoplasm and in ECM of healthy and tumor tissues. To distinguish between a cell and its surrounding ECM during the acquisition and the analysis of the bead motions, tissue samples were stained with a live-cell fluorescent dye to label nuclei (Hoechst 33342), as reported in the Materials and Methods section. In particular, as seen in Supplementary Fig. 1, when evaluating the trajectories of the beads inside the cells we considered those zones in which the cells are packed and the contributions of the ECM can be neglected (dotted blank square). Where this procedure was not feasible, we only considered those beads which are not more than 5 μm distant from the cell nuclei as belonging to the cell. Similarly, to determine the MSDs of the beads inside the ECM, we took advantage of the collagen autofluorescence and looked at those zones in which nuclei are absent or their contribution is fringe (dotted red square). In this analysis, healthy/tumor cells and stromal cells were not distinguished based on their morphological characteristics and specific functions. In fact, the purpose of this work was to evaluate the mechanical properties of the intra-cellular micro-environment by studying the collaborative and synergetic interactions between tumor and stromal cells in the emergence of the cancer.

Before performing the particle tracking analyses of *ex vivo* lung tissues, a Trypan Blue assay was used in order to evaluate the viability of tissues after cryopreservation. The tissue samples were rapidly thawed in a 37°C water bath, maintained in complete medium and stained with Trypan Blue. The results (not shown) suggest that post-thaw tissue viability was maintained when cryopreserved by using DMSO. We also compared MSDs of cryopreserved and 4% paraformaldehyde-fixed tissues. MSDs of fixed tissues were close to the noise floor and

appeared to flatten out, as consequence of cell death. On the contrary, MSDs of cryopreserved tissues indicated a sub-diffusive behavior, which originated from actin network confinement and cytoskeletal hindrance (Supplementary Fig. 2).

Mechanical comparisons of healthy and tumor lung tissue removed from each patient were performed. MPT analyses showed that the cancerous transformation of tissues had a remarkable effect on the dynamics of the tracer beads in tumor cells and their associated ECM (Fig. 1-2). This evidence, obtained from averaging all the *ex vivo* samples investigated with no distinction between grade and stage of tumor, was in line with well-established results *in vitro* and with more recent *ex vivo* comparisons [23, 24]. In particular, particles in cells of adenocarcinoma tissue exhibit greater MSDs amplitude at all explored lag times as compared to cells of normal tissue (Fig. 1a). The observed increased motion could be associated to a less structured cytoskeleton (in terms of polymerized actin bundles) and then to an increase in the compliance or deformability of cells, as already observed in 2D [11, 12] and 3D [25] *in vitro* systems. In fact, it was demonstrated that cell softening is strictly correlated with cancerous transformation, characterized by resistance to anoikis, cell anchorage-independent growth and the capability to migrate and invade distant tissues [26]. Furthermore, the onset of cancer is also characterized by a change in the mechanical properties of the extracellular-microenvironment, which becomes stiffer within malignant tissues. Indeed, MPT analyses revealed that MSDs in tumor ECM are smaller in comparison to normal tissue at all time lags (Fig. 1b). During the last years there has been a gradual accumulation of evidence suggesting that a stiffening of the ECM promotes cancer progression and cell transformation from normal to malignant to metastatic [19, 27, 28]. In particular, the enhancement of collagen cross-linking and consequently the ECM stiffness, results in increased integrin activity and focal adhesion signaling which promotes tumor

proliferation, survival and invasiveness [19].The alteration of integrin adhesions in malignancy are associated to the miR-18a circuit which is activated by tensile forces generated by stiffened ECM [29]. In fact, increased EMC stiffness influences miR-18a expression, leading to PI3K-dependent malignant progression [29].

Interestingly, we observed a statistically significant 2.5 times change in MSDs amplitude (Figs. 1a, b, and 2a, b) between the healthy and the tumor tissues. In particular, the mean square displacement was increased when nanobeads were embedded in the cells, whereas it decreased in the ECM. These findings suggest a sort of symmetric modification of the mechanical properties of the cells and the extra-cellular matrix caused by the onset of a tumor. Most unexpectedly, it was noted that cells in tumor tissues resulted as being more compliant although residing in a stiffer matrix. We do not know if the differences observed in compliance were associated to a damaged/compromised mechanosensing machinery in cancer cells. In order to more thoroughly investigate this aspect we cultured H522 cells from lung adenocarcinoma on polyacrylamide substrates which had different stiffnesses (see Supplementary Figs. 3 and 4). The polymeric substrates were fabricated by mimicking an ECM stiffening from 4 to 30 kPa and evaluating the cell spreading area at 24 and 48 hours. Cell spreading, in fact, represents a very good indicator of the mechanosensing process of cells [20]. H522 cells showed a different morphology on the substrates, with a higher spreading area on the stiffer substrate (30 kPa). From previous works it has been shown that the ability of mechanosensing may be different depending on the tumor cell line [30] and all the experimental evidence came from *in vitro* characterizations. H522 sense the stiffness of the polyacrylamide substrates which increases the cell area and reorganize their cytoskeleton when moving from 4 to 30 kPa. During *in vitro* experiments we were able to recreate some physiological conditions, but it is impossible to control and replicate them all. As

shown in the comparison between the mechanical behavior of cells in biopsy tissue and 2D culture, tumor cells could display different behaviors and characteristics, depending on the nature of the surrounding environment.

Different ECM organizations in tumor biopsies are also revealed in the actin, nuclei and collagen stained sections (Fig. 2c-l). The structural changes in tumor ECM architecture, which occur with transformation from healthy tissues to adenocarcinomas are clear. By combining confocal fluorescence and second harmonic generation (SHG), we investigated the spatial distribution of cells and collagen in normal and tumor samples. In normal lung tissues collagen fibers were curly, isotropically and uniformly distributed (Fig. 2d). In tumor tissues the bundles were thicker, linearized and presented a higher density, as the SHG reconstruction has higher average intensity (Fig. 2h). Such linear collagen bundles were the fibrous substrate on which cells could migrate at high velocity and with high persistence [31]. Moreover, cells were different in number and organization. Tumor slices presented a higher amount of cells which clumped in reservoirs between the collagen bundles. This was indicative of a different production and remodeling of ECM from normal and tumor cells and, consequently, as already confirmed from MPT analysis, different mechanical properties.

We also searched for a correlation between the nanomechanical properties of bioptic tissues and their grade and stage as they were defined by the most recent classification of lung tumors [32]. Unfortunately, samples of grade 1 were missing in the 10 sample patients we investigated (see Supplementary Table 1) but, as shown in Fig. 5a, we found a clear correlation between MSDs of cells and tumor grade. MSDs and cell deformability increase in a significant way when tumor grade passes from 2 to 3, resulting in about 2 to 5 times higher than normal tissues in the case of grade 2 and 3, respectively. It would be interesting in the future to establish if the progressive

softening of cells with increasing tumor grade could be ascribable to the trans-differentiation process during tumor advancement [33]. Conversely, Fig. 5b reports that the ECM stiffening process we registered of the passage from a normal tissue to a tumor tissue is not directly dependent on the tumor grade. Such findings are in agreement with tumor grading assessed by a conventional morphological procedure for lung tumor (Fig. 5c-h). In fact, it is based on how much tumor cells differ morphologically and grow faster than normal cells and not on the ECM structural changes which occur during tumor progression. In particular, the most important factor in grading analysis of lung adenocarcinoma is the degree of cytologic atypia, defined by nuclear pleomorphism and presence of distinct nucleoli. Fig. 5 shows representative H&E stained-sections of tumor of grade 2 and grade 3. In the case of grade 2 (Fig. 5c, e, g), the tumor shows a solid and glandular growth and cells with moderately pleomorphic nuclei and greater nucleus/cytoplasm ratio. The grade 3 tumor (Fig. 5d, f, h) presented almost entirely solid nests or cords of cells with very poorly pleomorphic nuclei and a variable quantity of cytoplasm. In addition, in the case of the grade 3 tumor, it is possible to observe a more abundant deposition of laminin around the tumor cell nests, confirming the observation of more bountiful ECM components that contribute to increase ECM stiffness.

Notwithstanding the grade, the stage of the tumor resulted correlated strictly with the mechanical properties of both cells and ECM. MSDs of NPs in cells significantly increased when the tumor advanced from stage 1 to stage 3 (Fig. 5i). Inversely, MSDs decreased sensitively in ECM from normal tissue to cancer at stages 1 and 3 (Fig. 5l). As in the case of the grade, the sample population lacked stage 2. A linear progression of the softening process which occurs during the trans-differentiation pathway of the tumor was observed by analyzing the mechanical properties of the cells. And, by comparing the MSDs of tumor tissues at stages 1 and 3 we found an

increase of 2.3 and 3.5 fold times for tumor cells compared to their healthy counterparts and a decrease of 2 and 4 fold times for ECM. As reported in the Supplementary Table. 1, at stage 1 tumor cells were not found in regional lymph nodes in any of the tissues (tumors were classified as N0), while in tumors at stage 3, N was assigned a value of 2, indicating that the tumor had spread to regional lymph nodes. Lymph node invasion represents one of the first steps in the pathogenesis of metastasis, increasing the probability of developing a secondary tumor [34, 35]. At variance with tumor grade, tumor stage is indeed representative of the capability of tumor cells to grow into the adjacent tissues (leading to the progressive increase in tumor size and the occurrence of extra-pulmonary extension upon contiguity) and to invade lymphatic nodes (leading to lymph node involvement) and/or blood vessels (leading to the development of distant metastases). In this context the correlation of mechanical properties of both cells and ECM with tumor stage is of particular interest since it appears to be linked to the "invasive" tumor cell characteristics. A recent study demonstrated that cancer cells which metastasized to the lymph nodes up-regulate most important ECM proteins, in particular collagen I fibers, forming a "freeway" for metastasis [36]. In particular, in the case of lung cancer, it was observed that an altered ECM cross-linking is found within lung cancer: high laminin-5 expression and Lysyl oxidase-mediated collagen cross-linking correlated with lung cancer invasiveness [37]. This result is consistent with our findings that tumor stage and cancer stiffening are closely associated.

Conclusions

Mechanical comparisons of healthy and tumor *ex vivo* samples (biopses) removed from 10 patients affected by adenocarcinoma of lung were studied. The mechanical characterization was

performed by introducing nanometric probes inside the tissues and analyzing their motion with MPT technique. Results showed that when tissues undergo to the cancerous transformation remarkable effects on the dynamics of the tracer beads in tumor cells and their associated ECM were detectable. A statistically significant 2.5 times variation in the mean square displacement amplitude of the nanoprobes was observed between the healthy and the tumor tissues. In particular, it increased when nanobeads were embedded in the cells and decreased in the ECM, suggesting an asymmetric modification of the mechanical properties of the cells and the extra-cellular matrix caused by the onset of the tumor and when the stage increases even though the cell resides in a stiffer matrix it is more compliant.. Finally, we also found a good correlation between the nanomechanical properties of bioptic tissues and the grade and stage of the tumor, evaluated by standard immunohistochemical procedure. While passing from grade 2 to 3, cell deformability increased resulting about 2 and 5 times higher than normal tissues, the ECM stiffening process showed no correlation with the tumor grade. We also found a strict correlation between the mechanical properties of both cells, ECM and tumor staging. These results, achieved in *ex vivo* environment, suggest additional considerations about the physical evolution of cells and the surrounding extracellular matrix when a neoplastic transformation arises and advances. This simultaneous mechanical phenotyping of cell and ECM offers new and alternative interpretations to the mechanobiology of cancer and may provide an efficient additional support in the diagnosis.

Supporting Information. Supportive image representative for cell and ECM classification during PTM experiments; supportive viability experiments of tissue in Figure 1; supportive mechano-sensing *in vitro* experiments on H522 tumor cell line. Representative image of

nanobead trajectories in healthy and tumor samples in Figure 5. Supportive co-variance tests were performed for two representative samples in Figure 6. Supportive information on parameters of classification of analyzed adenocarcinoma samples in Table 1.

Author Contributions

The study was conceived by S.F. and P.A.N. V.P. and S.F. designed the experiments and developed all the customized hardware and software solutions for MPT. I.M. performed morphological analysis. I.R. and M.V. performed the patho-histological analysis and provided human biopsies. V.P. and I.M. performed the MPT experiments. V.P., I.M. and S.F. analysed the MPT data. V.P. and S.F. wrote the paper. All authors discussed the results and commented on the manuscript. All authors have given approval to the final version of the manuscript.

Competing financial interest

The authors declare no competing financial interests.

Acknowledgment

The authors would like to thank Mrs R. Infranca for manuscript proofreading and editing.

Figure captions

Figure 1. Ensemble-averaged MSDs of 500 nm fluorescent particles in cells (a) and ECM (b) of healthy (blue line) and adenocarcinoma (red line) tissues. ***, $p<0.001$; $n>700$ for all studied cases.

Figure 2. (a,b) The average measured MSD at 1 second turned out to be 2.5 times higher in tumor cells than in healthy ones (a), indicating softening of the cell during cancerous

transformation. Contrarily, the decrease of MSD in tumor ECM indicated a matrix stiffening which in several ways promotes tumor progression. (c-l) Phalloidin staining of actin (magenta, c-g), collagen by second harmonic generation (SHG-white, d-h) and Hoechst staining of nuclei (green, e-i) of healthy (top) and tumor (bottom) lung biopsies. Scale bar, 50 μm.

Figure 3. Ensemble-averaged MSDs of 500 nm fluorescent particles in **cells** (a) and **ECM** (b) of healthy (blue line) and adenocarcinoma **grade 2** (red line) and **grade 3** (green line) tissues. **, $p<0.01$, ***, $p<0.001$; n between 200 and 600 for all studied cases.

Figure 4. Ensemble-averaged MSDs of 500 nm fluorescent particles in **cells** (a) and **ECM** (b) of healthy (blue line) and adenocarcinoma **stage 1** (red line) and **stage 3** (green line) tissues. **, $p<0.01$, ***, $p<0.001$; n between 200 and 700 for all studied cases.

Figure 5. (a, b) MSDs of nanoparticles (NPs) inside the cells correlated directly with tumor grade, increasing 2 and 5 fold for tumor grade 2 and 3, respectively (a). This finding indicates that cell compliance represents an important factor in the regulation of the trans-differentiation process. Contrarily, it seems that there is not a strict correlation between cancer grade (2 and 3) and matrix stiffening (b). (c-h) Adenocarcinoma tumors were stained with hematoxylin and eosin (H&E) (top) and laminin (bottom). Original magnification, 200× for all images. (c) H&E-stained section shows increased proliferation of epithelial cells and partial cell growth in tubular glands. (d) the H&E stained section shows the typical confluent solid growing nests of solid pattern cells. Laminin staining shows the deposition of new and more abundant membrane basement components around tumor cell nests in the case of a grade 3 tumor (f) compared to a grade 2 tumor (e). Scale bar is 400 μm. In (g-h) a greater magnification of laminin staining: scale bar is 100 μm. (i, l) Both MSDs of NPs inside the cells and in the ECM correlated directly with the

tumor stage. Cancer cell softening and ECM stiffening promote tumor invasiveness and the ability to metastasize lymph nodes and probably also other sites.

References

[1] Fletcher DA, Mullins RD. Cell mechanics and the cytoskeleton. Nature 2010;463:485-92.
[2] Connelly JT, Gautrot JE, Trappmann B, Tan DW-M, Donati G, Huck WT, Watt FM. Actin and serum response factor transduce physical cues from the microenvironment to regulate epidermal stem cell fate decisions. nature cell biology 2010;12:711-8.
[3] Yamaguchi H, Condeelis J. Regulation of the actin cytoskeleton in cancer cell migration and invasion. Biochimica et Biophysica Acta (BBA)-Molecular Cell Research 2007;1773:642-52.
[4] Comoglio PM, Trusolino L. Cancer: the matrix is now in control. Nature medicine 2005;11:1156-9.
[5] Yilmaz M, Christofori G. EMT, the cytoskeleton, and cancer cell invasion. Cancer and Metastasis Reviews 2009;28:15-33.
[6] Pathak A, Kumar S. Biophysical regulation of tumor cell invasion: moving beyond matrix stiffness. Integrative Biology 2011;3:267-78.
[7] Lin Z, Han Y, Wu B, Fang W. Altered cytoskeletal structures in transformed cells exhibiting obviously metastatic capabilities. Cell Research 1990;1:141-51.
[8] Panzetta V, De Menna M, Bucci D, Giovannini V, Pugliese M, Quarto M, Fusco S, Netti P. X-RAY IRRADIATION AFFECTS MORPHOLOGY, PROLIFERATION AND MIGRATION RATE OF HEALTHY AND CANCER CELLS. Journal of Mechanics in Medicine and Biology 2015;15:1540022.
[9] Raz A, Geiger B. Altered organization of cell-substrate contacts and membrane-associated cytoskeleton in tumor cell variants exhibiting different metastatic capabilities. Cancer Research 1982;42:5183-90.
[10] Panzetta V, De Menna M, Musella I, Pugliese M, Quarto M, Netti PA, Fusco S. X-rays effects on cytoskeleton mechanics of healthy and tumor cells. Cytoskeleton 2016.
[11] Cross SE, Jin Y-S, Rao J, Gimzewski JK. Nanomechanical analysis of cells from cancer patients. Nature nanotechnology 2007;2:780-3.
[12] Lekka M, Laidler P, Gil D, Lekki J, Stachura Z, Hrynkiewicz A. Elasticity of normal and cancerous human bladder cells studied by scanning force microscopy. European Biophysics Journal 1999;28:312-6.
[13] Cavallaro U, Christofori G. Cell adhesion and signalling by cadherins and Ig-CAMs in cancer. Nature Reviews Cancer 2004;4:118-32.
[14] Oka H, Shiozaki H, Kobayashi K, Inoue M, Tahara H, Kobayashi T, Takatsuka Y, Matsuyoshi N, Hirano S, Takeichi M. Expression of E-cadherin cell adhesion molecules in human breast cancer tissues and its relationship to metastasis. Cancer research 1993;53:1696-701.
[15] Volk T, Geiger B, Raz A. Motility and adhesive properties of high-and low-metastatic murine neoplastic cells. Cancer research 1984;44:811-24.

[16] Egeblad M, Werb Z. New functions for the matrix metalloproteinases in cancer progression. Nature Reviews Cancer 2002;2:161-74.
[17] Deryugina EI, Quigley JP. Matrix metalloproteinases and tumor metastasis. Cancer and Metastasis Reviews 2006;25:9-34.
[18] Malik R, Lelkes PI, Cukierman E. Biomechanical and biochemical remodeling of stromal extracellular matrix in cancer. Trends in biotechnology 2015;33:230-6.
[19] Levental KR, Yu H, Kass L, Lakins JN, Egeblad M, Erler JT, Fong SF, Csiszar K, Giaccia A, Weninger W. Matrix crosslinking forces tumor progression by enhancing integrin signaling. Cell 2009;139:891-906.
[20] Fusco S, Panzetta V, Embrione V, Netti PA. Crosstalk between focal adhesions and material mechanical properties governs cell mechanics and functions. Acta biomaterialia 2015;23:63-71.
[21] Tseng Y, Kole TP, Wirtz D. Micromechanical mapping of live cells by multiple-particle-tracking microrheology. Biophysical journal 2002;83:3162-76.
[22] Hoffman BD, Massiera G, Van Citters KM, Crocker JC. The consensus mechanics of cultured mammalian cells. Proceedings of the National Academy of Sciences 2006;103:10259-64.
[23] Tian M, Li Y, Liu W, Jin L, Jiang X, Wang X, Ding Z, Peng Y, Zhou J, Fan J. The nanomechanical signature of liver cancer tissues and its molecular origin. Nanoscale 2015;7:12998-3010.
[24] Plodinec M, Loparic M, Monnier CA, Obermann EC, Zanetti-Dallenbach R, Oertle P, Hyotyla JT, Aebi U, Bentires-Alj M, Lim RY. The nanomechanical signature of breast cancer. Nature nanotechnology 2012;7:757-65.
[25] Baker EL, Lu J, Yu D, Bonnecaze RT, Zaman MH. Cancer cell stiffness: integrated roles of three-dimensional matrix stiffness and transforming potential. Biophysical journal 2010;99:2048-57.
[26] Liotta LA, Kohn E. Anoikis: cancer and the homeless cell. Nature 2004;430:973-4.
[27] Paszek MJ, Zahir N, Johnson KR, Lakins JN, Rozenberg GI, Gefen A, Reinhart-King CA, Margulies SS, Dembo M, Boettiger D. Tensional homeostasis and the malignant phenotype. Cancer cell 2005;8:241-54.
[28] Provenzano PP, Inman DR, Eliceiri KW, Knittel JG, Yan L, Rueden CT, White JG, Keely PJ. Collagen density promotes mammary tumor initiation and progression. BMC medicine 2008;6:11.
[29] Mouw JK, Yui Y, Damiano L, Bainer RO, Lakins JN, Acerbi I, Ou G, Wijekoon AC, Levental KR, Gilbert PM. Tissue mechanics modulate microRNA-dependent PTEN expression to regulate malignant progression. Nature medicine 2014;20:360-7.
[30] Li J, Wu Y, Schimmel N, Al-Ameen MA, Ghosh G. Breast cancer cells mechanosensing in engineered matrices: Correlation with aggressive phenotype. Journal of the mechanical behavior of biomedical materials 2016;61:208-20.
[31] Condeelis J, Segall JE. Intravital imaging of cell movement in tumours. Nature Reviews Cancer 2003;3:921-30.
[32] Travis WD, Brambilla E, Burke AP, Marx A, Nicholson AG. Introduction to The 2015 World Health Organization Classification of Tumors of the Lung, Pleura, Thymus, and Heart. Journal of Thoracic Oncology 2015;10:1240-2.
[33] Thiery JP. Epithelial–mesenchymal transitions in tumour progression. Nature Reviews Cancer 2002;2:442-54.

[34] Alitalo K, Tammela T, Petrova TV. Lymphangiogenesis in development and human disease. Nature 2005;438:946-53.
[35] Gupta GP, Massagué J. Cancer metastasis: building a framework. Cell 2006;127:679-95.
[36] Rizwan A, Bulte C, Kalaichelvan A, Cheng M, Krishnamachary B, Bhujwalla ZM, Jiang L, Glunde K. Metastatic breast cancer cells in lymph nodes increase nodal collagen density. Scientific reports 2015;5.
[37] Wood SL, Pernemalm M, Crosbie PA, Whetton AD. The role of the tumor-microenvironment in lung cancer-metastasis and its relationship to potential therapeutic targets. Cancer treatment reviews 2014;40:558-66.

Figura 1

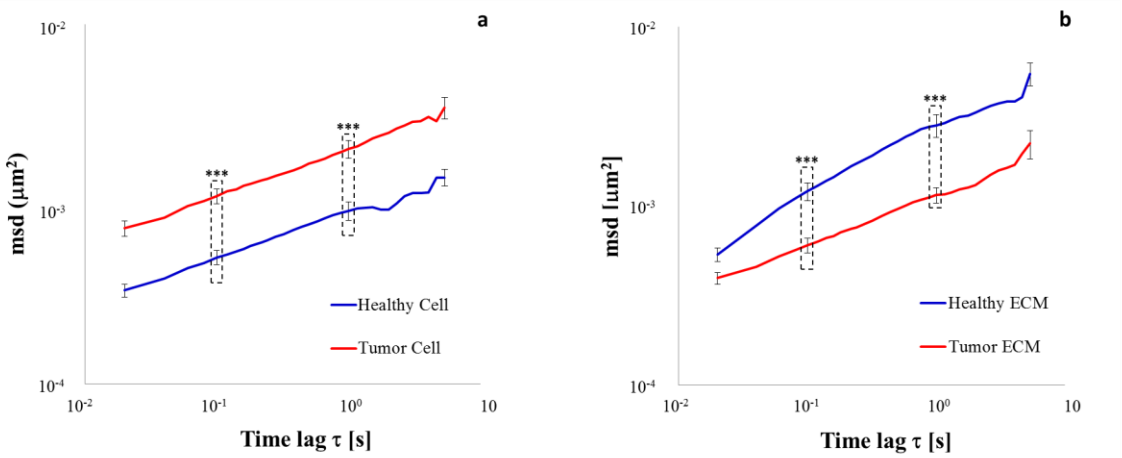

Figura 2

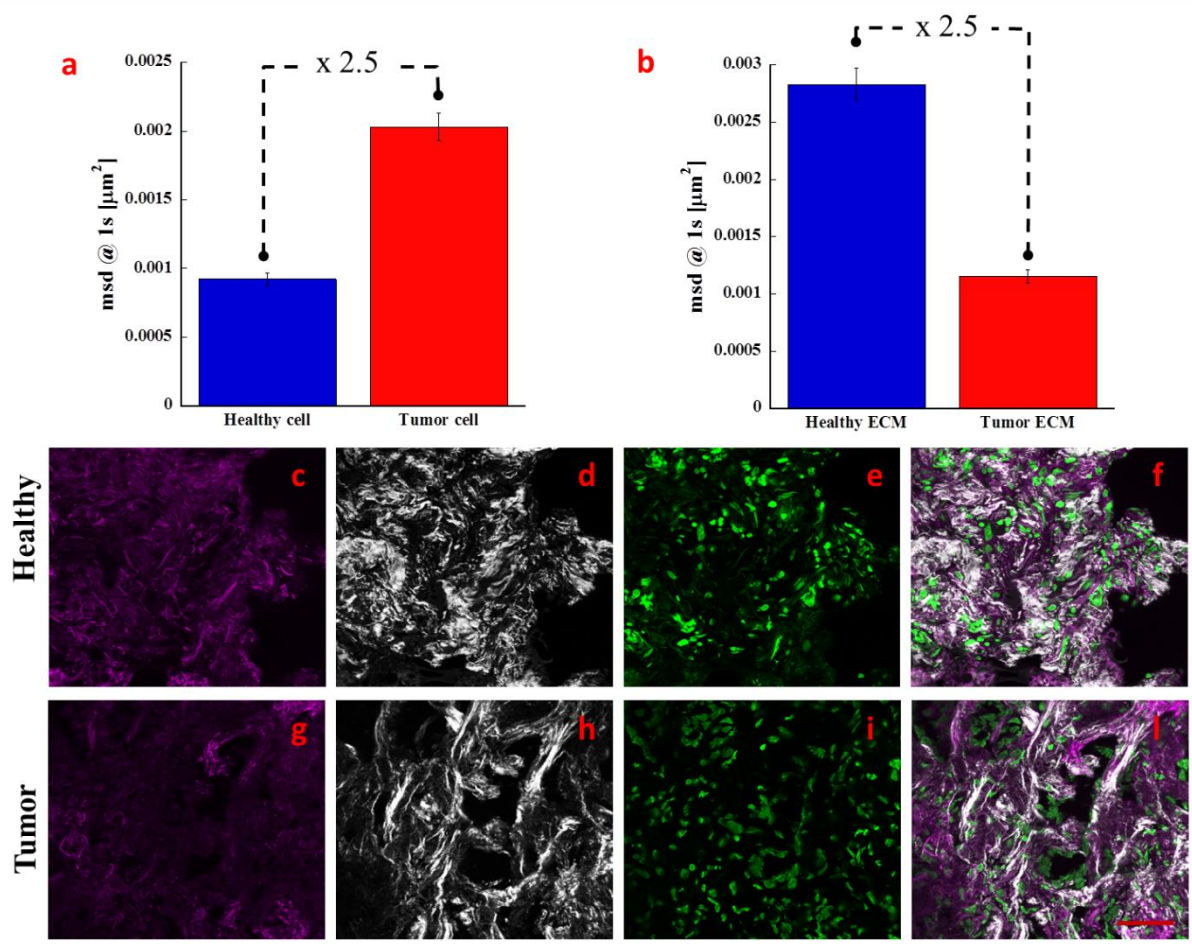

Figura 3

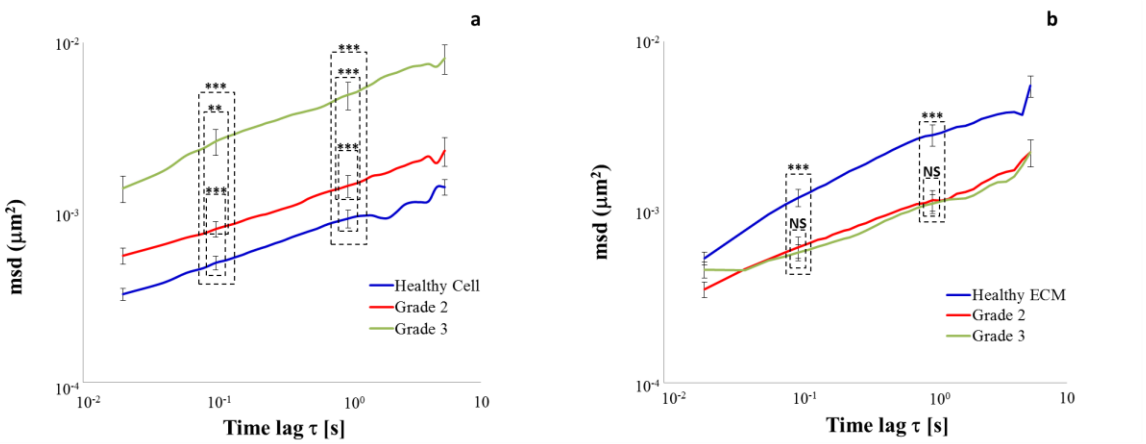

Figura 4

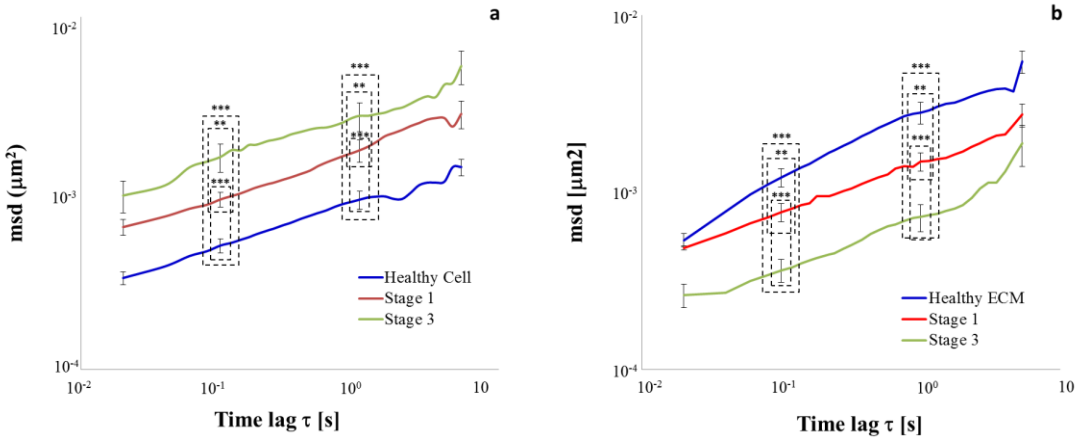

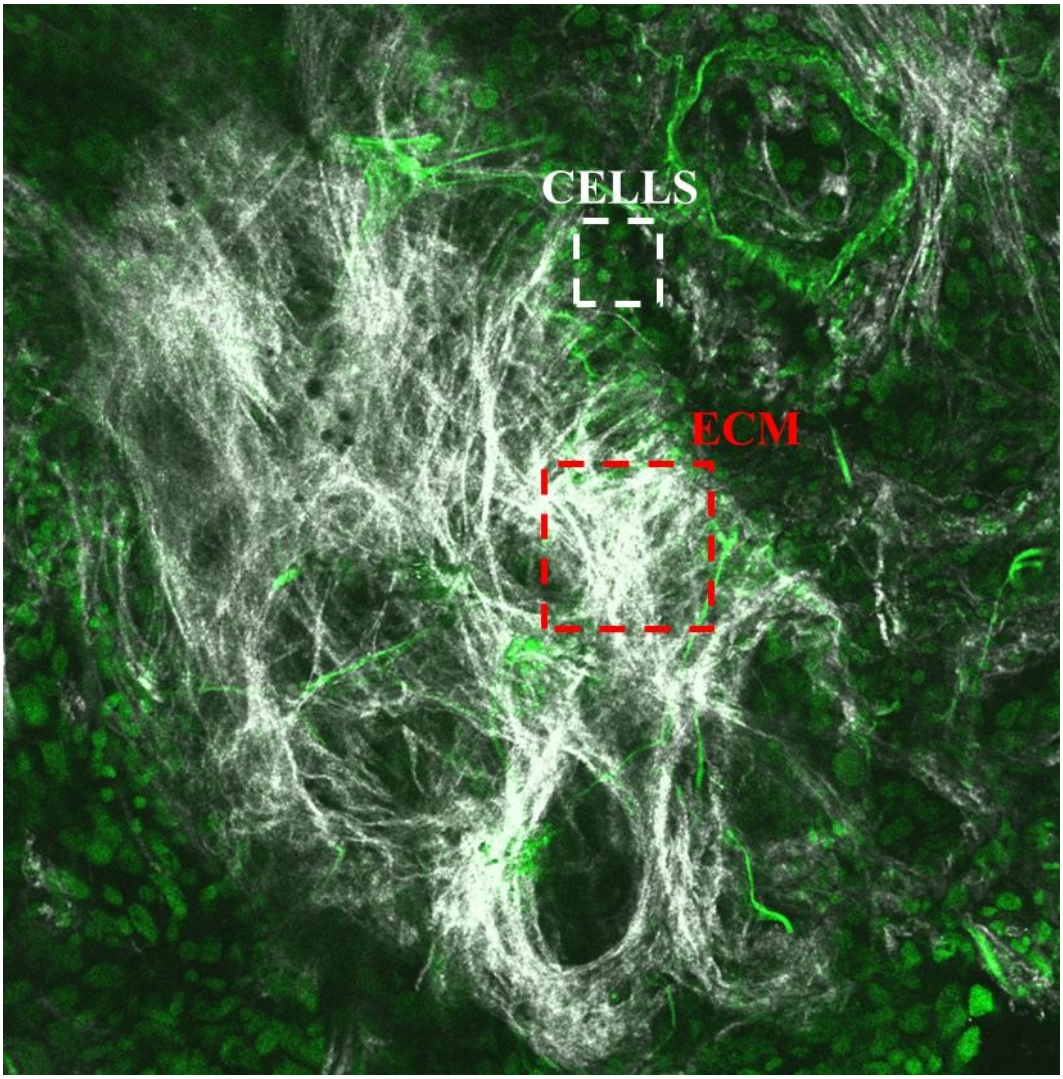

Supplementary Figure 1. The particles were considered inside the cells when they are in those zones in which the cells are packed and the contributions of the ECM can be neglected (dotted blank square). Where this procedure was not feasible, we only considered those beads which are not more than 5 mm distant from the cell nuclei as belonging to the cells. Similarly, to determine the MSDs of the beads inside the ECM, we took advantage of the collagen autofluorescence and looked at those zones in which nuclei are absent or their contribution is fringe (dotted red square).